Jagadeep Thota, 2025, 13:5
ISSN (Online): 2348-4098
ISSN (Print): 2395-4752

International Journal of Science, Engineering and Technology
An Open Access Journal

Testing Sustainable Material for Aerospace Application

Jagadeep Thota[1], Ellyssa Purdy[2]
[1]Associate Professor, Mechanical Engineering, University of Wisconsin-Green Bay, Wisconsin, USA, thotaj@uwgb.com
[2]Student, Mechanical Engineering, University of Wisconsin-Green Bay, Wisconsin, USA, purdem15@uwgb.edu

Abstract- Aerospace vehicles, such as a rocket, need to be light weight. They carry heavy payloads and critical flight instrumentation (avionics) which need to be protected. Typically, aerospace vehicles contain single use parts, some of which may be made of even nylon and polystyrene, that are not environmentally friendly. Such materials can harm soils and the ecosystems upon disposal. This paper looks at replacing some of these aerospace vehicle parts, mainly the parts protecting the rocket avionics, by a sustainable biodegradable material. This study looks at the performance of the rocket avionics when enclosed by such sustainable material. The work presented in this paper involves utilizing computer-aided design (CAD) modeling coupled with numerical flight simulation. The aerospace vehicle, with the sustainable material parts, is flight tested.

Keywords: sustainability, biodegradable material, rocket, and flight testing.

I. INTRODUCTION

In an aerospace vehicle, like a high-powered rocket, enclosing critical components in protective material is crucial, as it maintains internal environments of avionics-bays (a-bays) and protects payloads from various harmful variables [1, 2]. In this work, the aerospace vehicle (or the flight configuration) is a single stage, dual-deploy, high-powered rocket designed to evaluate the performance of the flight avionics and internal parameters when enclosed by a sustainable biodegradable material [3, 4]. The propulsion system, consisting singularly of an Aerotech High Power Single Use Disposable Motor System (DMS) – J270W-P, is responsible for delivering the thrust required to attain target apogee for the rocket.

The recovery systems deploy the drogue and main parachutes when commanded by the motor delay charge and flight avionics. The flight avionics are responsible for ensuring the safe recovery of the rocket by monitoring the external conditions through instruments such as a barometer, accelerometer, and gyrometer. The Internal Data Acquisition System (IDAS) is responsible for monitoring the internal pressure, temperature, and humidity of the a-bay, as well as the external temperature, during flight [5-7]. The data obtained from this research work contributes to the optimization of the sustainable material for aerospace application.

In the next section, the paper introduces the rocket flight configuration or the major parts of the rocket used for conducting the flight test of the sustainable biodegradable material. Then the paper details the setup of the biodegradable material in the rocket. The latter section describes the various motors typically used to propel the high-powered rockets, and the one selected for the work presented in this paper. The section before the discussion of the results and conclusion summary, the flight avionics, i.e., the data measuring instruments/sensors, and the data acquisition system are described. The objective of this study is to check if the biodegradable material used in this work can provide a sustainable alternative for high-powered rocket parts.

II. ROCKET FLIGHT CONFIGURATION

The external rocket body was fabricated in accordance with the Tripoli Rocketry Association standards using filament wound G10-fiberglass material. SolidWorks, a three-dimensional CAD software, allowed preliminary spatial planning and design of parts. The internal rocket parts were subsequently rapid prototyped (3D printed) out of acrylonitrile butadiene styrene (ABS) material. Serially, from the rocket tip-to-tail was the sustainer section, a-bay, and booster section, as shown in

Figure 1. The sustainer section housed the main recovery subassembly and comprised of an ogive nosecone, nosecone bulkplate, nosecone coupler, and sustainer body tube. The mass housing, shown in Figure 2, which was also 3D printed, added 435 g of weight to the forward end of the nosecone bulkplate for stability. The rocket was 1.67 m tall, with the center of gravity and center of pressure located 1.16 m and 1.40 m, respectively, from the tip of the nosecone. This yielded a stability of 2.41 calibers. The rocket weighed 3.191 kg with the propulsion system, producing a thrust-to-weight ratio of 11:1.

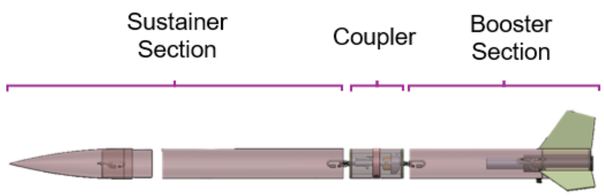

Figure 1: 3D model of the rocket with the three sections

The a-bay coupler houses the sled, biodegradable material, flight avionics, and IDAS, and is temporarily fixed to the sustainer and booster sections during the ascent phase of the rocket flight test. The avionics sled, shown in Figure 2, was 3D printed, and it provided the structural integrity to mount the flight avionics and IDAS instrumentation.

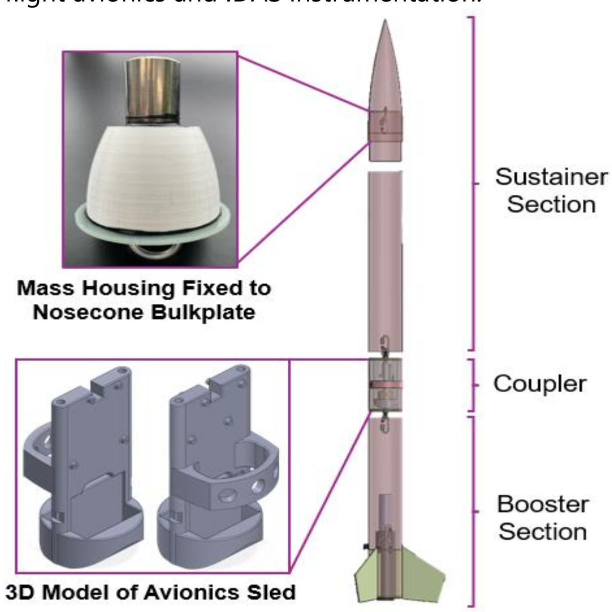

Figure 2: Showing the location of the mass housing and the avionics sled in the rocket

The booster section, which comprised of the booster body tube, forward and aft centering rings, motor mount tube (MMT), motor retainer with adaptor, and fins, supported the propulsion system and housed the drogue recovery subassembly. The internal aft end of the booster body tube housed two centering rings to maintain the installation of the MMT.

An aluminum, 54-to-38 mm, adaptor was inserted into the MMT. External to the booster body tube were three G10-fiberglass through-the-wall fins. High-strength epoxy was used to permanently bond the fiberglass components together. Eyebolts were installed in the bulkplates and forward centering ring for the recovery system attachment. Table 1 provides the dimensional parameters of the cylindrical and ogive components utilized in the computational methodology. In this table, ‘M’ is the mass of the rocket components, ‘LT’ is the length or thickness of the components, ‘OD’ and ‘ID’ are outer and inner diameters, respectively, of the rocket components.

Table -1: Dimensional parameters of the rocket components

Component	M (g)	LT (mm)	OD (mm)	ID (mm)
A-bay coupler	214.4	175	99	95
Aft bulkplate	70.8	5	99	95
Aft centering ring	25.1	3	99	58
Booster body tube	555.8	558.8	102	99
Forward bulkplate	69.9	5	99	95
Forward centering ring	25.1	3	99	58
Motor mount tube	91.4	225	57	54
Motor retainer adaptor	117.6	91	54	38
Nosecone	340.2	419	102	99
Nosecone bulkplate	43.7	3	95	-
Nosecone coupler	192.2	165	99	95
Sustainer	566.6	558.8	102	99
Switch band	26.4	23	102	99

2.1 Biodegradable Material Setup

The biodegradable material is a potato thermoplastic starch aerogel material developed by researchers at Purdue University and Indiana University, in USA [8]. For the rocket flight test, the avionics sled was wrapped in this biodegradable material. The IDAS instrumentation was ensured to be enclosed by the biodegradable material, while the rotary switches remained exposed. The biodegradable material was secured around the sled by a biodegradable masking tape. This setup is shown in Figure 3. This wrapped up avionics sled is placed within the a-bay coupler shown in Figure 4.

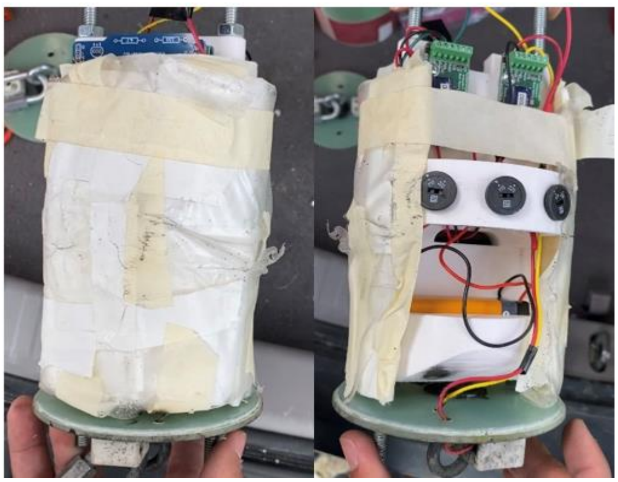

Figure 3: Biodegradable material enclosing the avionics sled with the instrumentation

Figure 4: The a-bay coupler (on the left) which will house the biodegradable material enclosed sled (on the right)

2.2 Rocket Propulsion System

The optimal propulsion system was the motor that could provide the longest flight (test) duration. Flight simulations were done using RockSim, a numerical flight simulation program, to predict the performance of the flight configuration when propelled by Aerotech 54 mm and 38 mm DMS motors. Table 2 shows the simulated results of these motors. The J270W was selected as the optimal motor as it provided the second longest predicted flight duration under ideal weather conditions and was easily available for purchase from off-the-shelf than the J435WS motor.

Table -2: Predicted performance of DMS motors for rocket propulsion

Motor Type	Altitude (m)	Apogee Time (s)	Flight Time (s)
I500T-P	1131.32	14.35	75.02
J270W-P	1288.96	15.59	81.61
I280DM-P	959.14	13.75	70.04
I65W-0	1057.94	16.29	74.41
J435WS-P	1467.27	15.98	87.07
I140W-P	406.14	10.43	51.83
I175WS-P	406.99	10.22	51.81

Ejection charges, which were small canisters of black powder, pressurized the booster and sustainer sections when ignited by the flight avionics. This subsequently deployed the recovery (drogue and main) parachutes. Hogdon FFFg muzzleloading powder was used as the propellant. Two sets of three M2x7.94-mm shear pins were installed to temporarily fix the sustainer and booster sections to the a-bay. An individual shear pin was able to resist a maximum load of 204.6 N.

Thus, one set of shear pins required a minimum load of 613.8 N to shear. To account for any additional forces during flight, the load considered was 667.2 N. The pressure required to deploy the parachutes was determined by taking the ratio of the load to the inner cross-sectional area of the body tubes, which resulted in 86.9 kPa. The amount of propellant required was determined using Equation 1 [9]. This resulted in 1.32 g and 1.64 g for drogue and main deployments, respectively. When conducting the ground and flight testing, each canister contained two grams of black powder, resulting in successful deployments.

BP = 5.16 x 10-4PV (1)

where,

BP = black powder (g)

P = pressure = 86.9 kPa

V = volume of the section = 0.004 m3 (drogue) and 0.003 m3 (main)

2.3 Simulation Flight Test

Prior to conducting the practical flight test, a 1.52 m launch guide was angled 2-degrees into the wind to ensure safe liftoff in the presence of excessive wind speeds [3]. A simulation of the flight was generated using the selected propulsion system and typical weather conditions, and comparing altitude, velocity, and acceleration to the flight duration, as shown in Figure 5. From Figure 5 graph, it was observed that the flight configuration was expected to depart the launch guide at 35.80 m/s and reach an altitude of 1194.81 m after 14.97 s, indicating safe stability at departure. A DMS delay drilling tool was utilized to shorten the delay element by two seconds to account for environmental conditions. During the powered ascent, the flight configuration experienced weather cocking because of the nosecone mass, reducing the altitude.

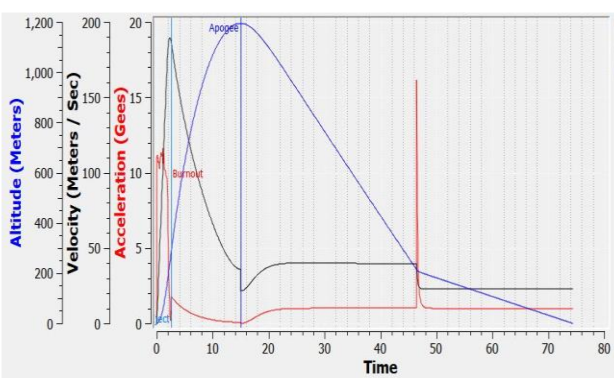

Figure 5: Simulated flight performance using Aerotech DMS J270 motor

2.4 Flight Avionics

The flight avionics consisted of autonomous primary and secondary subsystems. Each of these was comprised of a Blue Raven Altimeter, 9 V power source, and a rotary switch. The subsystems were responsible for triggering the drogue and main parachutes deployments at apogee and 213.36 m, respectively. This was done with the usage of measuring instruments such as barometers, accelerometers, and gyrometers.

Each altimeter was connected to a drogue and main ejection charge through terminal blocks on the coupler bulkplate. For drogue deployment redundancy, a motor delay charge of 12 seconds was implemented into the propulsion system. During the flight test, the flight avionics deployed the drogue and main recovery parachutes as intended. Upon retrieval of the tested rocket, following the second flight test, an anomaly occurred resulting in the deletion of the flight data from both the recovery subsystems.

The Internal Data Acquisition System (IDAS) was designed to measure and record pressure, temperature, and humidity during flight. A BME680 sensor served to measure the internal pressure, temperature, and humidity of the a-bay, while a DS18B20 sensor served to measure the external temperature. An Arduino Uno microprocessor with a sampling rate of one sample per second was used to collect data. This data was stored on a microSD card.

For this to happen a microSD card breakout board had to be used. The IDAS Printed Circuit Board (PCB), shown in Figure 6, served as a medium to connect the BME680, DS18B20, and microSD card breakout board to the Arduino Uno. A rotary switch controlled the power supply from a 9 V battery to the system. A wired DS18B20 connection broke during the flight test, preventing it from recording the external temperature. Other than this, the IDAS performed as intended during both the flight tests.

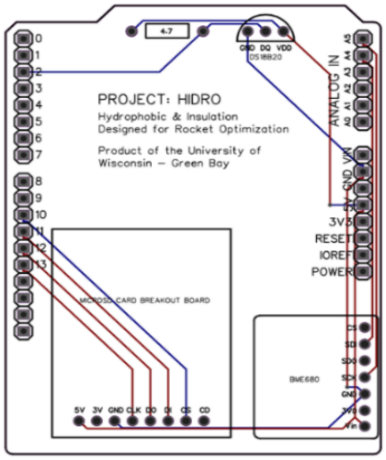

Figure 6: IDAS PCB architecture design

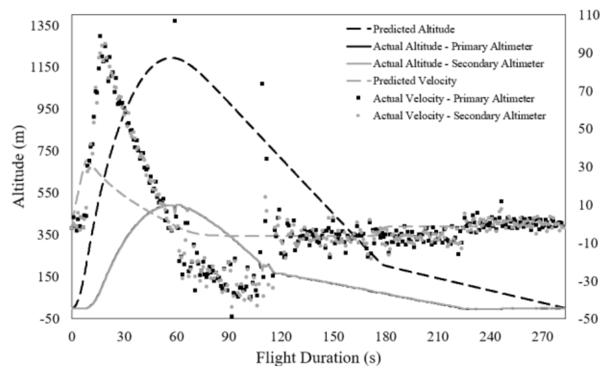

Figure 7: Comparing predicted and experimental flight test one performance

III. RESULTS AND DISCUSSION

The effect of the biodegradable material, when enclosing flight avionics, was determined by analyzing the variation between predicted and actual flight performance as well as internal and external parameter datasets. Comparisons between predicted altitude and velocity versus actual altitude and velocity for the first flight test are shown in Figure 7.

The actual altitude was measured to be 493.93 m, presenting discrepancy between the predicted and actual altitudes. Due to choking of the drogue parachute, the flight test exceeded the drogue target descent rate. Following the main parachute deployment, the flight configuration descended at a rate of 7.22 m/s

The performance of the flight avionics was determined to be unaffected by the biodegradable material encasing it, yielding safe descents for both the flight tests. The significant variation between predicted and actual altitudes is due to the result of exaggerated weathercocking caused by the high rate of wind present while testing. No variations in the comparisons of flight performance could be attributed to the addition of the biodegradable material. The low density and low weight of the biodegradable material created negligible impacts on the actual flight performance.

The environmental variance imposed upon the a-bay was determined by comparing the internal and external parameters. From Figure 8, it can be observed that at apogee, the second flight experienced a greater drop in pressure than the first flight. This was a result of the biodegradable material being damaged after the first flight test when the rocket impacted with the ground at the end of the test. As some sections of the biodegradable material were fractured, after the first test, the ability of this material to properly form a seal between the sled and a-bay coupler decreased.

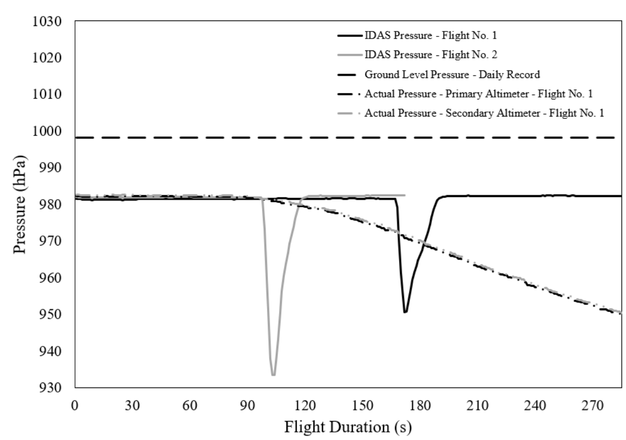

Figure 8: Comparing internal and external pressure data

Successful protection from thermal and humidity variance was observed due to the biodegradable material. As seen in Figure 9, due to the aforementioned fractures in the biodegradable material after the first flight test, the first flight exhibited significant mitigation to temperature variations in comparison to the second flight. The biodegradable material's ability to decelerate the rate of thermal changes demonstrated its credibility as a thermal insulator.

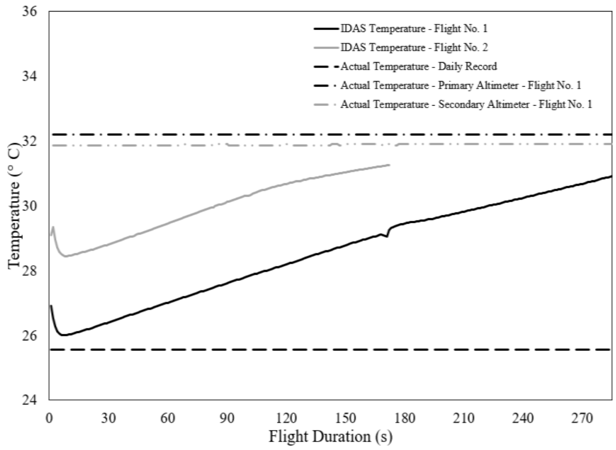

Figure 9: Comparing internal and external temperature

According to the humidity comparisons, shown in Figure 10, lower humidity levels were observed in the a-bay during the second flight compared to the first, presenting an inverse to the trends previously described. The cause was assumed to be the result of the fractured biodegradable material allowing internal airflow, consequently "drying" the internal environment of the a-bay. This finding corresponds to the observations and discussion surrounding pressure and temperature variations.

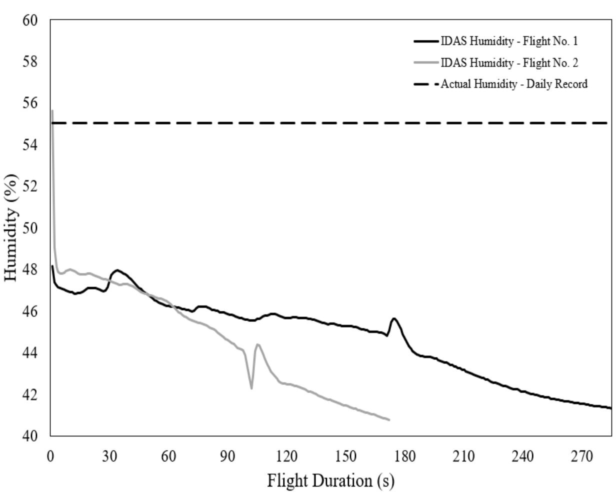

Figure 10: Comparing internal and external humidity data

IV. CONCLUSION

A study was conducted to determine the impact of using a sustainable biodegradable material in a single-stage, dual-deploy, high-powered rocket. The results showed that the incorporation of the biodegradable material provided protection for the flight avionics from humidity and temperature variation. The biodegradable material addition did not hinder the flight performance. Therefore, this research showed that the biodegradable material yielded a more promising and sustainable alternative, and a light weight option, to typical non-environmentally friendly materials used in such rocket parts and aerospace applications. Figure 11 shows the rocket which was flight tested with the biodegradable material encasing the avionics.

Figure 11: Rocket with the biodegradable material which was flight tested

Future work being done in this area of study:

- Check the potential sustainable usage of the biodegradable material for other parts of the rocket.
- Reuse the biodegradable material parts for multiple flight tests.

Acknowledgements

The authors gratefully acknowledge the collaborators and organizations whose support and contributions directly impacted the success of this research. Gratitude to the NASA Wisconsin Space Grant Consortium for their financial support. Thanks to the College of Science, Engineering and Technology at University of Wisconsin-Green Bay for providing financial assistance to conduct the experiments. Special thanks are due to Purdue University and Indiana University, USA, for supplying the biodegradable material.

REFERENCES

1. Bhat BN (2018) Aerospace materials and applications. Aerospace Research Central, https://doi.org/10.2514/4.104893
2. Meador MAB, Aleman CR, Hanson K, Ramirez N, Vivod SL, Wilmoth N, McCorkle L (2015) Polyimide aerogels with amide cross-links: a low cost alternative for mechanically strong polymer aerogels. ACS Applied Materials & Interfaces, 7(2), 1240-1249.
3. Paulson P, Curtis J, Bartel E, Cyr WO, Lamsal C (2017) High powered rocketry: design, construction, and launching experience and analysis. Physics Education, 53(1) https://doi.org/10.1088/1361-6552/aa90fc
4. Calcara LE, Fernandez M, Green C, Hosokawa T (2016) High power rocket design report. Honors Thesis, Loyola Marymount University, Los Angeles, CA.
5. McWhorter P (2014) Arduino Lesson 21: Log sensor data to an SD card. Toptechboy.com
6. Santos S (2020) Guide for BME680 environmental sensor with Arduino (gas, temperature, humidity, pressure). Random Nerd Tutorials.
7. Ada L (2024) Micro SD card breakout board tutorial. Adafruit Industries.
8. Staker J, Schott S, Singh R, Collier K, Druschel G, Siegel A, Tovar A (2024) Influence of choline chloride/urea and glycerol plasticizers on the mechanical properties of thermoplastic starch plastics. Polymers, 16(6), 751. https://doi.org/10.3390/polym16060751
9. Cavender D (2015) NASA high power rocketry video series counterpart documents. National Aeronautics and Space Administration (NP-2015-09-84-MSFC)